Correlations of long-lived chemical species in a middle atmosphere general circulation model

Correlations of long-lived chemical species in a middle atmosphere general circulation model

David Sankey and Theodore G. Shepherd
Department of Physics, University of Toronto, Toronto, Ontario, Canada

Received 25 July 2002; revised 8 February 2003; accepted 12 March 2003; published 19 August 2003.

[1] Correlations between various chemical species simulated by the Canadian Middle Atmosphere Model, a general circulation model with fully interactive chemistry, are considered in order to investigate the general conditions under which compact correlations can be expected to form. At the same time, the analysis serves to validate the model. The results are compared to previous work on this subject, both from theoretical studies and from atmospheric measurements made from space and from aircraft. The results highlight the importance of having a data set with good spatial coverage when working with correlations and provide a background against which the compactness of correlations obtained from atmospheric measurements can be confirmed. It is shown that for long-lived species, distinct correlations are found in the model in the tropics, the extratropics, and the Antarctic winter vortex. Under these conditions, sparse sampling such as arises from occultation instruments is nevertheless suitable to define a chemical correlation within each region even from a single day of measurements, provided a sufficient range of mixing ratio values is sampled. In practice, this means a large vertical extent, though the requirements are less stringent at more poleward latitudes. *INDEX TERMS:* 0341 Atmospheric Composition and Structure: Middle atmosphere—constituent transport and chemistry (3334); 3319 Meteorology and Atmospheric Dynamics: General circulation; 3334 Meteorology and Atmospheric Dynamics: Middle atmosphere dynamics (0341, 0342); *KEYWORDS:* chemical correlations, long-lived species, transport and mixing

Citation: Sankey, D., and T. G. Shepherd, Correlations of long-lived chemical species in a middle atmosphere general circulation model, *J. Geophys. Res.*, *108*(D16), 4494, doi:10.1029/2002JD002799, 2003.

1. Introduction

[2] Chemical species in the atmosphere undergo advection by time-dependent wind patterns. As a result, point measurements of chemical species exhibit short-term variability which can be thought of as uninteresting "noise" on their long-term time evolution. Because different long-lived species are advected in a similar manner, correlation plots between chemical species are unaffected by advection and provide a way of eliminating dynamical variability from the measurements. *Roach* [1962] first noticed that such a plot of O_3 versus H_2O during a stratospheric sudden warming showed a relation between the two species, rather than a space-filling scatterplot, and *Allam et al.* [1981] found a similar relation between O_3 and H_2O using a troposphere-stratosphere general circulation model (GCM). Although the O_3:H_2O relation is generally not compact, *Ehhalt et al.* [1983] observed compact correlations between various long-lived chemical species using stratospheric observations.

[3] The existence of compact correlations between chemical species was given a theoretical basis in the work of *Mahlman et al.* [1986] and *Holton* [1986], who investigated the transport of chemical species in a simple one-dimensional chemical transport model of the troposphere and stratosphere. *Plumb and Ko* [1992] generalized their work to a two-dimensional zonally averaged model of the lower and middle atmosphere. A three-dimensional modeling study was performed by *Avallone and Prather* [1997], who considered the existence of correlations between various long-lived chlorine- and bromine-containing species and N_2O.

[4] In addition to the modeling work, recent measurement campaigns have begun to provide much data, and a great deal of published work has confirmed that compact correlations between chemical species can be observed in the atmosphere [e.g., *Loewenstein et al.*, 1993; *Michelsen et al.*, 1998a, 1998b]. *Kelly et al.* [1989] initiated the widespread use of correlations between chemical species using data from the Airborne Antarctic Ozone Experiment (AAOE), and since then many other studies have used correlations to infer and attempt to quantify various properties of the atmospheric circulation, both chemical and dynamical. For example, *Proffitt et al.* [1989] used correlations between O_3, N_2O and NO_y using data obtained from the AAOE campaign to investigate chemical O_3 loss in and around the Antarctic polar vortex. Similar work was performed by *Proffitt et al.* [1990] for the Arctic polar vortex, and followed up by *Müller et al.* [1996], who used the correla-

0148-0227/03/2002JD002799$09.00

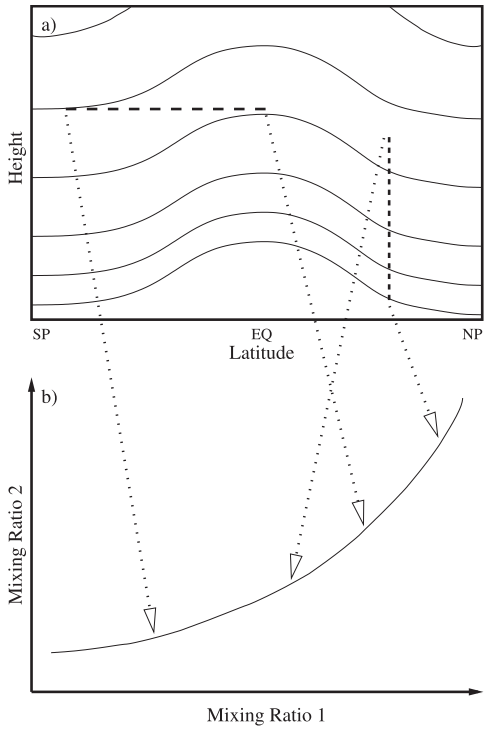

Figure 1. (a) Typical mixing ratio isopleths for a chemical tracer with a surface source and an upper atmosphere sink (e.g., N_2O, CH_4, CFCs). The mixing ratio decreases with altitude. (b) Correlation diagram between two such chemical species, showing how sampling different regions of the atmosphere produces different portions of a single correlation curve.

tion between CH_4 and O_3 for the same purpose. Correlations have also been used to investigate the tropical pipe [*Plumb*, 1996]: *Murphy et al.* [1993] used the correlation between O_3 and NO_y to locate the boundaries of the tropical pipe, and *Volk et al.* [1996], *Minschwaner et al.* [1996], and *Avallone and Prather* [1996] used various correlations to quantify the leakiness of the tropical pipe in the lower stratosphere. *Boering et al.* [1994] used the correlation between CO_2 and N_2O to investigate the extent to which the tropospheric seasonal cycle of CO_2 propagates into the lower stratosphere. All these investigations have used either satellite or aircraft measurements as the source of their observations, except for *Michelsen et al.* [1998a, 1998b] who used Atmospheric Trace Molecule Spectroscopy (ATMOS) data from the space shuttle.

[5] In this paper we present a series of chemical correlation plots based on results from the Canadian Middle Atmosphere Model (CMAM), which is a fully interactive chemistry climate model. The purpose of the study is twofold. The first is to characterize the chemical climate of the model and assess the extent to which it seems realistic, with a particular focus on transport properties. The second is to use the model as a way of testing the existence of different correlations and their degree of compactness. This has already been done with 2D models [e.g., *Plumb and Ko*, 1992], but not very extensively with 3D models. *Hall and Prather* [1995] considered only correlations between CO_2, N_2O and O_3 using the Goddard Institute for Space Studies GCM, and *Plumb et al.* [2000] used a 3D model, although not a GCM, to investigate the effects of the polar vortex mixing barrier on correlations. By using the results from this study we can learn more about the use of certain correlations as a diagnostic. In particular, limited sampling from satellite or aircraft measurements could lead to artificially compact correlations, and the adequacy of such sampling can be tested with the model.

[6] The outline of the paper is as follows. In section 2 we review the basic reasons why compact correlations are expected to exist for long-lived species, closely following the work of *Holton* [1986] and *Plumb and Ko* [1992]. Section 3 gives a brief overview of the CMAM. Section 4 presents some basic correlations to show that the CMAM data is producing expected results, before presenting the evolution of several correlations through a typical year of the model run. Conclusions and a discussion are presented in section 5.

2. Basis for Compact Correlations Between Long-Lived Chemical Species

[7] Point measurements of chemical species whose lifetimes are longer than several days exhibit much variability due to short-term meteorological fluctuations. However, such fluctuations move air parcels around coherently, meaning that any correlations that exist between two species will persist despite the fluctuations. Thus examining correlations rather than point measurements provides a way to eliminate the effects of short-term dynamical variability

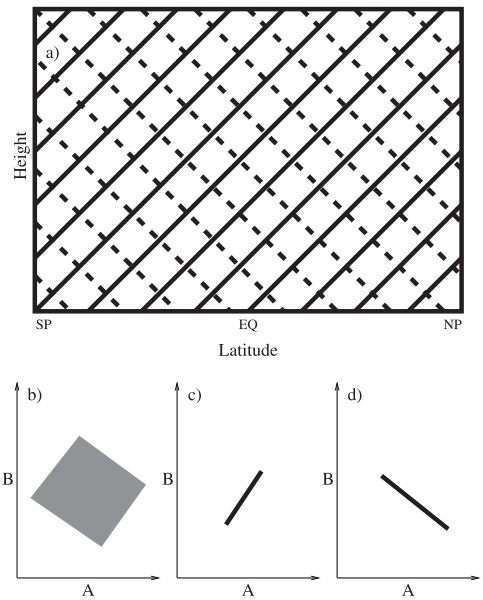

Figure 2. (a) Mixing ratio isopleths of two hypothetical uncorrelated tracers A (solid lines) and B (dashed lines). The mixing ratio of A decreases from bottom-right to top-left, and the mixing ratio of B decreases from bottom-left to top-right. (b) Correlation plot obtained from sampling the whole atmosphere. (c) Correlation plot obtained from a single vertical sample. (d) Correlation plot obtained from a single horizontal sample.

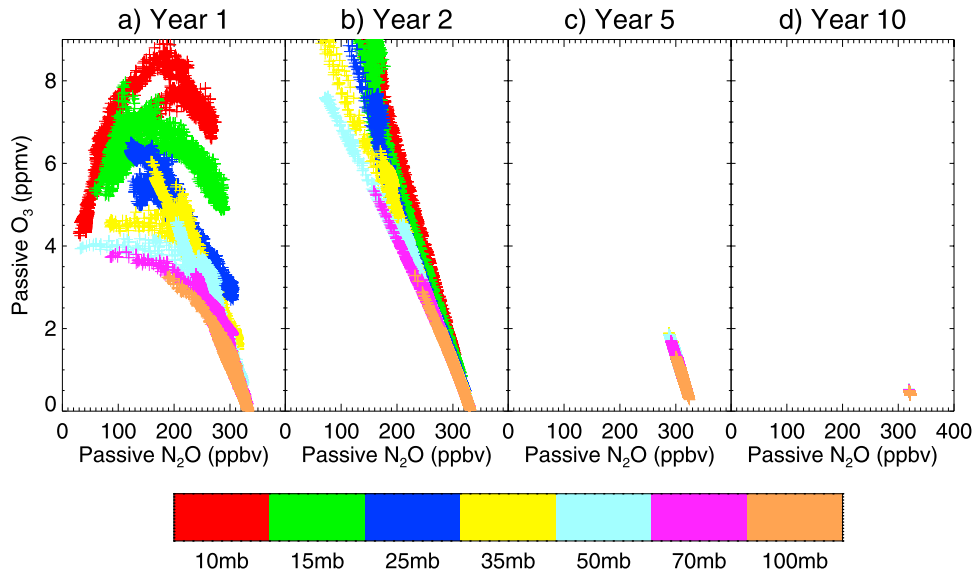

Figure 3. (a–d) Time evolution of a passive O_3 versus passive N_2O correlation. The tracers are initialized with the spatial distributions of N_2O and O_3, and then advected by the model winds without chemistry. The latitudinal extent of the data is from the south pole to the north pole, and the pressure levels are color-coded as shown.

from chemical measurements [*Ehhalt et al.*, 1983]. Species whose lifetimes are longer than several weeks become reasonably well-mixed in the horizontal by isentropic motions, and therefore tend to have quasi-horizontal mixing ratio isopleths. Their meridional-vertical distribution then represents a balance between the slope-steepening effect of differential vertical advection (by the diabatic circulation) and the slope-flattening effect of isentropic mixing [*Mahlman et al.*, 1986; *Holton*, 1986]. This accounts for the characteristic meridional distribution of N_2O, CH_4, etc. as seen in observations [e.g., *Randel et al.*, 1993] and as sketched in Figure 1a.

[8] When such conditions prevail, mixing ratio isopleths of different long-lived chemical species coincide. Scatterplots then give a compact correlation. A vertical section of measurements (e.g., from a balloon, ground-based sensor or satellite sounding) and a horizontal section (e.g., from an aircraft) will sample different parts of this single correlation, but have to give consistent results (see Figure 1b).

[9] For very long-lived chemical species the slope of the correlation curve is independent of altitude and the correlation is linear. For intermediate lifetimes (longer than the several-week mixing time on an isentropic surface, but shorter than the several-year timescale of the diabatic circulation) the correlation is nonlinear [*Plumb and Ko*, 1992]. So the slope of the correlation depends on chemistry, but the existence of a correlation in the first place is the result of dynamics.

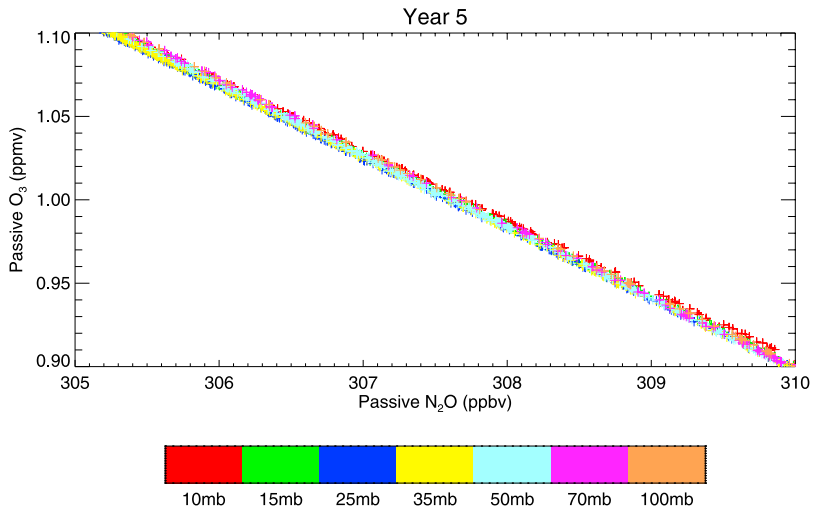

Figure 4. Blow-up of the passive O_3 versus passive N_2O correlation for year 5 of the CMAM run. See text for more details.

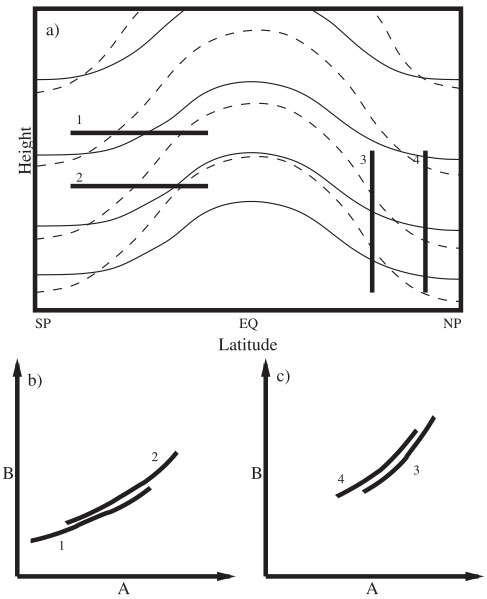

Figure 5. (a) Mixing ratio isopleths for two hypothetical species A (dashed lines) and B (thin solid lines). The mixing ratio of both species decreases with altitude. (b) Striations in the correlation plot obtained by taking two horizontal samples, labeled 1 and 2. (c) Striations in the correlation plot obtained by taking two vertical samples, labeled 3 and 4. Note that the same value of B corresponds to a higher value of A in 1 than in 2, and in 3 than in 4.

[10] It is sometimes incorrectly stated that compact correlations depend on chemistry. For two species converted between each other but otherwise long-lived, one obtains a compact anti-correlation arising from chemistry: An example is CH_4 and H_2O in the stratosphere. However, such cases are rare. In the more general case where the extent of a chemical conversion depends on various factors such as temperature and there are other products (e.g., N_2O to NO_y), there would be an anti-correlation in the statistical sense, but it would not be compact. Any compactness (e.g., in the case of N_2O and NO_y, discussed further in section 4) arises from dynamics.

[11] Another point is that if two species are not correlated, then single sections in height or latitude will show apparent correlations, but these are not compact correlations in the sense we mean (see Figure 2). Rather, they are an artifact of the reduced dimensionality of the data set.

3. Methodology

[12] The chemical correlations presented in this paper are calculated from simulations made with the Canadian Middle Atmosphere Model (CMAM), which is a comprehensive GCM incorporating radiation, interactive chemistry, gravity-wave drag, surface exchanges of heat, moisture and momentum, as well as many other physical processes. The winds and chemical transport are calculated using a T32 spectral method, while the chemical reactions and physical processes are calculated on an associated linear Gaussian transform grid of 64 $\times$ 32 points (a grid spacing of approximately 5.625°). In the vertical the model ranges from the surface of the earth to approximately 96 km, having 50 layers of unequal thickness spanning this interval, with approximately a 3 km vertical spacing in the middle atmosphere. In the runs used in this paper a total of 36 different chemical species or families are advected, and 95 gas-phase chemical reactions are calculated (heterogeneous reactions are not included). The vertical diffusion rate of the chemical species, K_{zz}, is set to 1 $m^2\ s^{-1}$; although this might be considered a little high, it gives realistic column O_3 amounts throughout the year. For more details about the dynamical aspects of the CMAM, see *Beagley et al.* [1997], and for more details about the chemical aspects, see *de Grandpré et al.* [1997]. Long-term simulations with fully interactive chemistry are described by *de Grandpré et al.* [2000].

[13] The correlation diagrams presented in the following sections were constructed as follows. At the particular time step of interest, samples of the chemical species in question were taken from the output data of the CMAM. These included vertical samples and horizontal samples, although the precise latitudinal and longitudinal extent of the sampling varied (details are given in the figure captions). The resulting "measurements" were then plotted against each other to produce the correlation plot. In general, the plots are color-coded according to the model pressure level from which the data were taken, and all correspond to a single model time step.

4. Correlations

[14] This section details the correlations between various chemical species in the CMAM at different times of the year, and investigates the conditions under which we can expect the correlations to be compact. Unless stated otherwise, the correlations shown are all taken from the 24th year of the model run in order to allow for quasi-steady correlations to be observed.

4.1. Passive Versus Passive

[15] We first consider the most basic of correlations: that between two passive tracers. One is initialized as N_2O and the other initialized as O_3. After the start of the model run these two species undergo no chemical reactions, and their spatial distributions are thereafter affected only through advection by the model winds and numerical diffusion.

[16] According to the theory laid out by *Holton* [1986] and *Plumb and Ko* [1992], tracers with extremely long lifetimes produce a special type of compact correlation, called "slope equilibrium," characterized by a straight-line correlation. Since the two passive tracers have an infinite lifetime, they ought to produce a correlation of the slope-equilibrium type. Figure 3 shows the evolution of the correlation between these two passive tracers as the model run progresses, with the color-coding corresponding to the different pressure levels at which the "measurements" have been taken. Initially, in the first year of the model run, there is no correlation between the two tracers as their mixing ratios still closely resemble those of the species with which they were initialized. Since the chemical lifetime of O_3 is relatively short we cannot expect an O_3-like tracer to have a compact correlation with a long-lived species such as N_2O at the initial time. This is reflected in the fact that the spatial distribution of O_3 is completely different from that of N_2O.

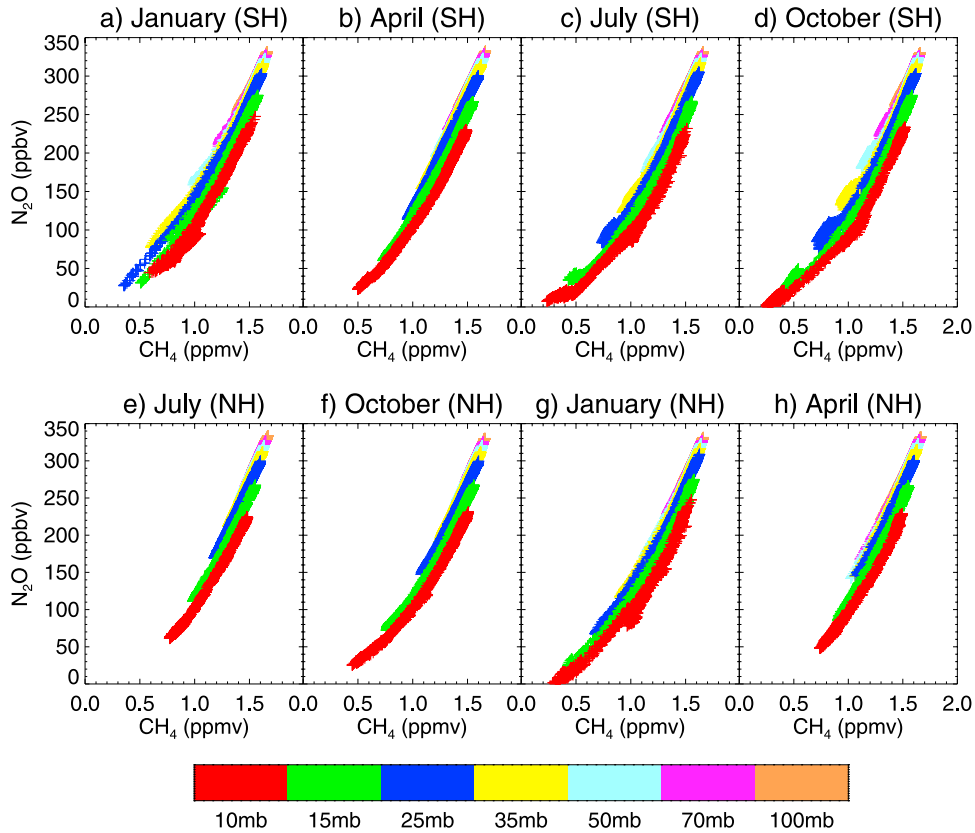

Figure 6. N_2O versus CH_4 throughout the year. The correlations for the Southern Hemisphere (90S to the EQ) for (a) January, (b) April, (c) July and (d) October are shown in the top row. The correlations for the Northern Hemisphere (EQ to 90N) for (e) July, (f) October, (g) January and (h) April are shown in the bottom row. The pressure levels are color-coded as shown.

[17] However, as the model run progresses, we can see that even by year 2 of the run a compact correlation is beginning to form as the tracers lose knowledge of their initial state and are advected and diffused by the dynamics of the model. By year 5 the compact correlation is very strong, and by year 10 the tracers have become virtually uniformly mixed throughout the whole model atmosphere, resulting in a correlation plot that is almost a point in mixing ratio space.

[18] It is interesting to note, however, that even for such infinitely long-lived tracers it is impossible to obtain a perfectly compact correlation. Figure 4 shows a blow-up of year 5 of the correlation between the two passive tracers. Although in Figure 3 it appears that a compact correlation has formed, examination of Figure 4 reveals that there is a striated pattern in the correlation picture, with the points at the different altitudes not lying exactly on top of each other. The striations occur at all times and are also observed in correlations between other species.

[19] The striations arise from the finite width of the correlations combined with the discrete vertical resolution of the model. For the passive tracers the finite width is a finite-time effect. For real chemical species it reflects the finite lifetimes [*Plumb and Ko*, 1992]. Thus the mixing ratio isopleths are never perfectly aligned. The effect is illustrated in Figure 5. Consider two chemical species A and B which both decrease with altitude, but suppose that the meridional slope of A is slightly steeper than the slope of B (A is the dashed line in Figure 5). Then for a given value of B, A is higher at higher altitudes. This gives rise (Figure 5b) to the parallel striations seen in Figure 4. Similarly, for a given value of B, A is lower at higher latitudes. So vertical soundings lead to striations too, although at a different angle (Figure 5c).

4.2. N_2O Versus CH_4

[20] We next consider two active chemical species with long (but not infinite) lifetimes, CH_4 and N_2O. In this case we expect a compact correlation to exist, although perhaps no longer a straight-line slope-equilibrium correlation as seen in Figure 4 for the passive tracers. The structure of the correlation between these two species for the months of January, April, July and October is shown in Figure 6 for both hemispheres, offset by 6 months to allow for easier comparison. In spite of the finite lifetime of these two species, the correlations between CH_4 and N_2O are reasonably compact. As expected, the striations found in the plots for the passive tracers can be seen here in all months.

[21] Overall there is very little variation in the correlation between these two chemical species throughout the year. The most noticeable seasonal variation is the lower values of the two species found in the winter middle stratosphere (the red points in Figures 6c, 6d, and 6g). These lower

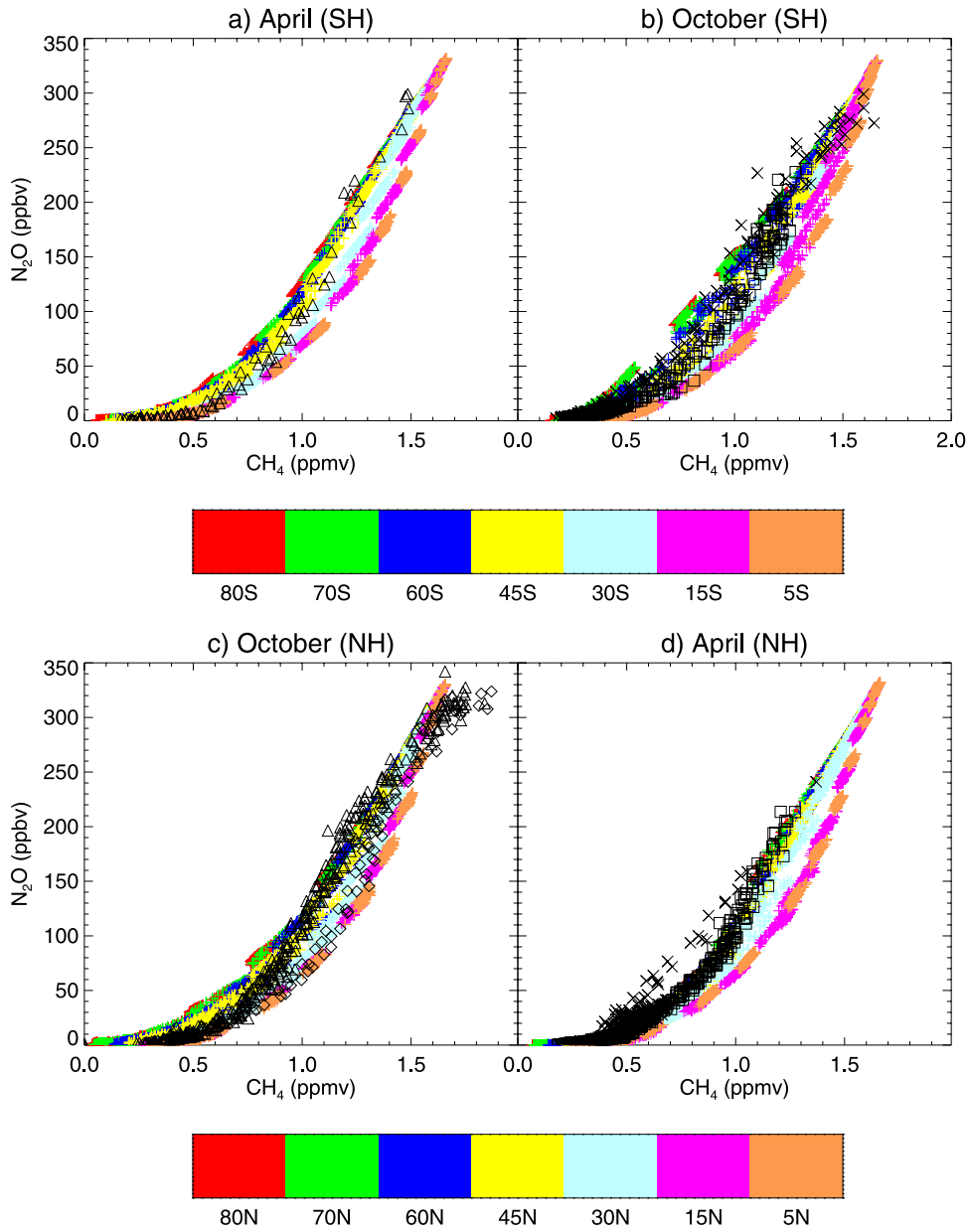

Figure 7. N_2O versus CH_4 in the Southern Hemisphere for (a) April and (b) October, and in the Northern Hemisphere for (c) October and (d) April. The color-coding shows the latitude at which the vertical sections were taken. In the vertical the data lie between 100mb and 0.3mb. The black symbols represent data from Plate 2 of *Michelsen et al.* [1998b], with diamonds showing tropical data, squares showing midlatitude data, triangles high-latitude data, and crosses vortex data.

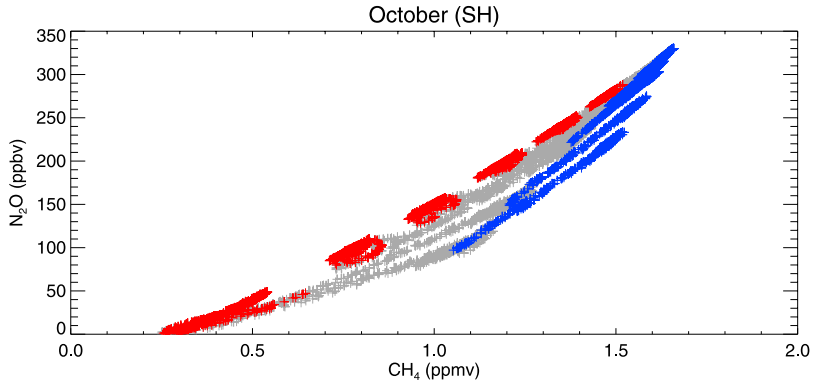

Figure 8. N_2O versus CH_4 in the Southern Hemisphere for the first day of October. The latitudinal extent of the data runs from 90S to the EQ, and the vertical extent from 100mb to 10mb. The red points denote data between 90S and 70S, the gray points denote data between 70S and 20S, and the blue points denote data between 20S and the EQ.

values are the result of air from above being drawn downward inside the winter polar vortex.

[22] The correlation plots in Figure 6 were produced by taking horizontal samples of the species along various pressure surfaces. Figure 7 shows corresponding correlation plots for April and October generated by taking vertical samples along various latitude bands. Also shown in Figure 7 are ATMOS data from Plate 2 of *Michelsen et al.* [1998b], labeled by latitude (see figure caption for details). The overall structure of the plots is similar to those in Figure 6, and again we see the striations due to the slight misalignment of the tracer mixing ratio isopleths for the two species. The patterns of the striations in Figures 6 and 7 correspond well to the expected patterns sketched in Figures 5b and 5c, respectively.

[23] However, in Figure 7 we see not just striations, but distinct structures in the correlations, separated by gaps. The theory of *Plumb and Ko* [1992] summarized in section 2 assumes no mixing barriers. In the real atmosphere, this is obviously not the case—there are several well-known mixing barriers, including the tropical pipe [*Plumb*, 1996] and the polar vortex barrier during the winter-spring season. While the theoretical understanding of the effect of mixing barriers on chemical correlations is incomplete, *Plumb et al.* [2000; see also *Plumb*, 2002] argue that the air on either side of a mixing barrier is ascending or descending at different rates and that the "leakiness" of the barrier allows air from different regions of the correlation diagram space to mix, producing an "anomalous correlation." This manifests itself as a different curve on the correlation diagram.

[24] There are several distinct correlations evident in Figure 7 in both the CMAM and ATMOS data. The tropical correlations (orange and magenta points and diamonds) are distinct from the midlatitude correlations, particularly for CMAM in Figures 7b and 7d (Southern Hemisphere and Northern Hemisphere spring), while in Figure 7b (Southern Hemisphere spring) the correlations in the Antarctic polar vortex (red and green points and crosses) are distinct from

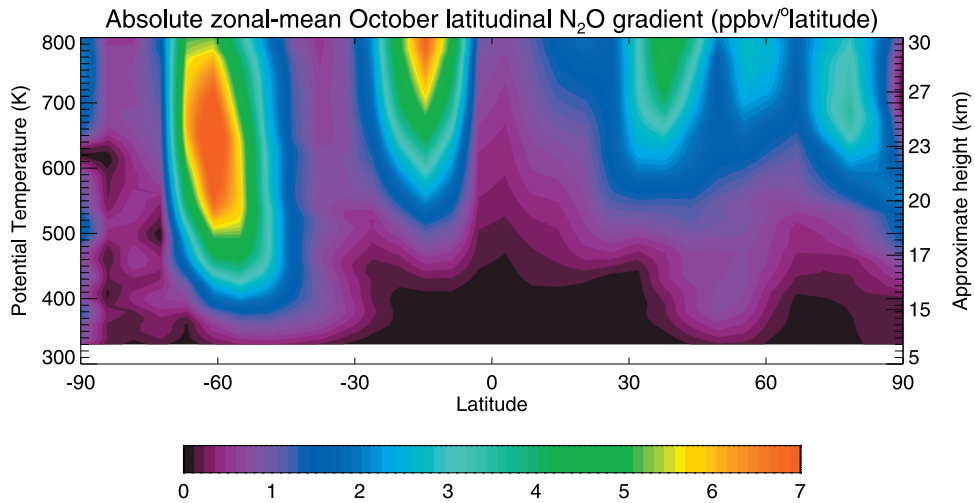

Figure 9. Absolute value of the zonal-mean latitudinal gradient of N_2O for October. The dark colors show low latitudinal gradients of N_2O, while the bright colors show large latitudinal gradients representing jumps in the mixing ratio across a mixing barrier.

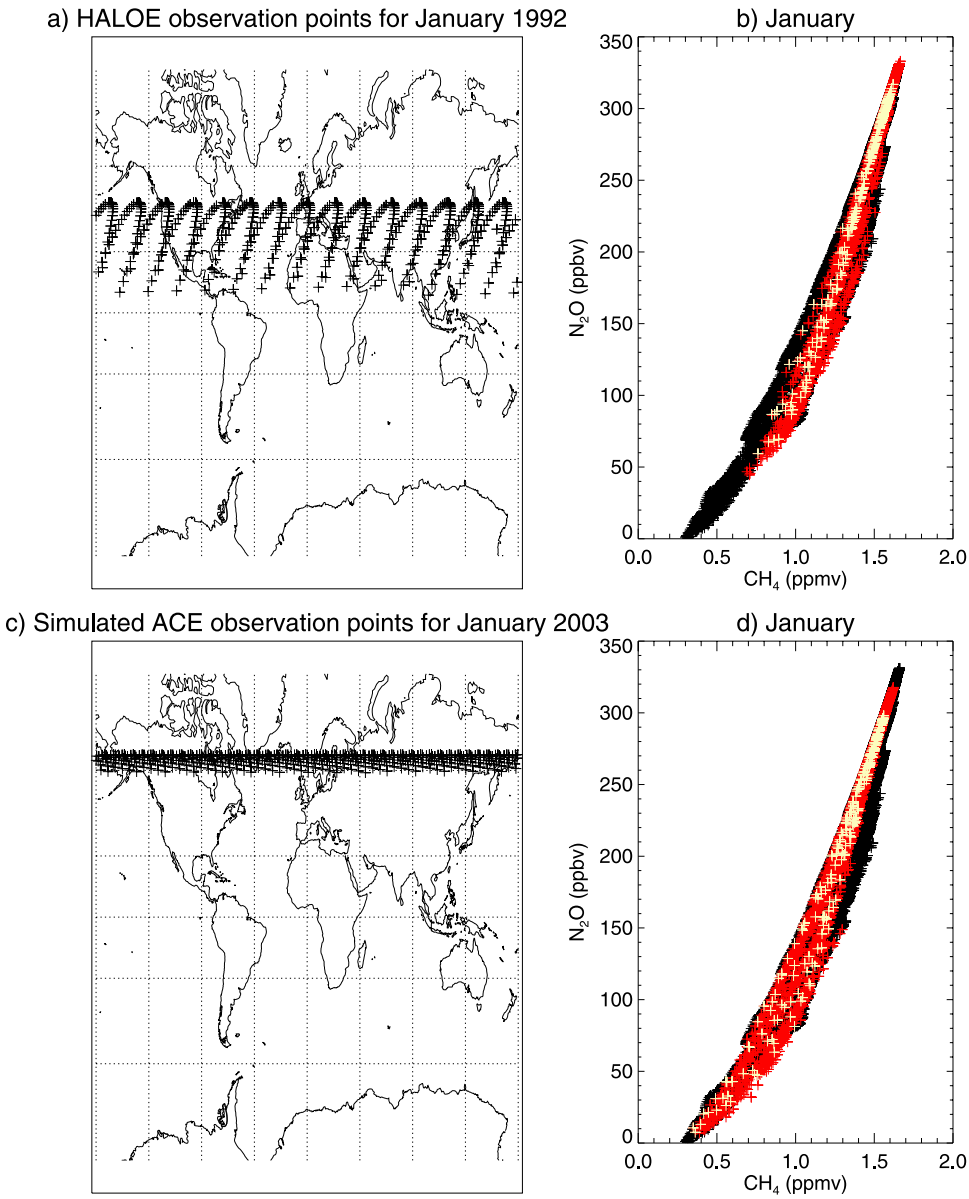

Figure 10. (a) The location of HALOE samplings at sunrise for January 1992. (b) Correlation between N_2O versus CH_4 from the CMAM (black points), from a month of HALOE samplings (red points) and from HALOE samplings on 16 January (yellow points). (c) Location of the ACE sampling points from a simulation. (d) As Figure 10b but for ACE.

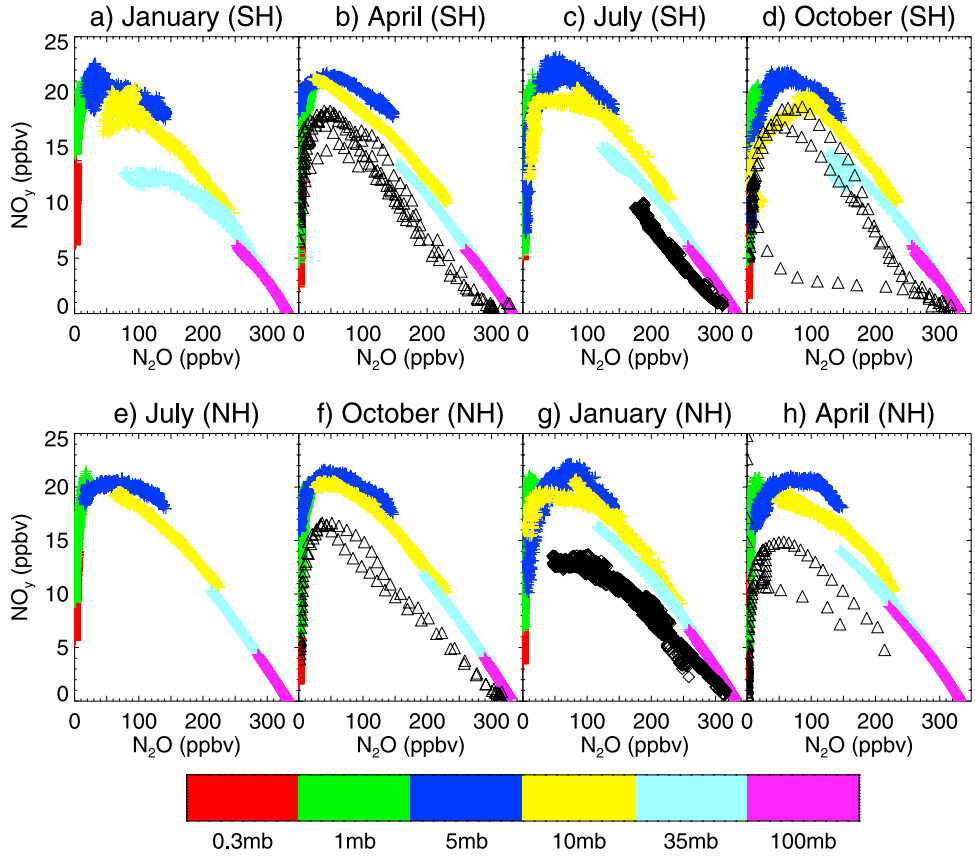

Figure 11. NO_y versus N_2O throughout the year. The correlations for the Southern Hemisphere (90S to the EQ) for (a) January, (b) April, (c) July and (d) October are shown in the top row. The correlations for the Northern Hemisphere (EQ to 90N) for (e) July, (f) October, (g) January and (h) April are shown in the bottom row. The pressure levels are color-coded as shown; the range is more extensive than in the other figures in order to compare with the data at higher altitudes. The triangles show data from Plate 1 of *Michelsen et al.* [1998b] and the diamonds show data from Figure 1 and Plate 3 of *Strahan* [1999].

the midlatitude correlations. With the exception of the Arctic vortex correlation (discussed further below), the CMAM and ATMOS data agree well within each of these distinct correlation regimes, where observational data exist.

[25] To highlight the distinct correlations more clearly, Figure 8 shows the identical correlation plot between N_2O and CH_4 for CMAM for the month of October (as in Figure 7b), but color-coded differently. Here, the points are labeled by their tropical, midlatitude or vortex location rather than by their individual latitude. The red points denote data between 90S and 70S, the gray points denote data between 70S and 20S, and the blue points denote data from 20S to the equator. It is clear from this figure that even though there are distinct correlations in these three different regions, the correlations in the tropics and midlatitudes still exhibit a finite amount of spreading due to the finite lifetimes of the two species. The correlation in the vortex is much more compact.

[26] In principle, we might expect a similar anomalous correlation in the correlation plot for April in Figure 7d due to the Arctic polar vortex, but evidently this is not the case for CMAM. In the CMAM, as in the real atmosphere, the winds at the Arctic polar vortex edge are much weaker than those at the Antarctic polar vortex edge, yielding a much weaker mixing barrier. In fact the lack of an anomalous correlation suggests that there is virtually no barrier at all in the CMAM Arctic vortex, and that the original theory of *Plumb and Ko* [1992] would therefore be more applicable in this region than that of *Plumb et al.* [2000]. The anomalous correlation can, in contrast, be clearly seen in the observational data from *Michelsen et al.* [1998b] (the black crosses in Figure 7d). The data are from April 1993, a year with very low total ozone in the Arctic spring, which suggests a particularly well defined Arctic vortex mixing barrier existed that year. The occurrence of such anomalously strong Arctic vortices does not appear to be a characteristic of this version of the CMAM.

[27] The distinction between the tropical and midlatitude correlations arises from the existence of mixing barriers at the edge of the tropical pipe. The location of the tropical pipe in the CMAM can be found by considering the zonal-mean latitudinal gradient of N_2O on isentropic surfaces. Figure 9 shows a color-coded contour plot of the absolute value of the zonal-mean latitudinal gradient of N_2O from 330K up to 800K. The brighter areas show regions of relatively large latitudinal gradient and thus likely correspond to mixing barriers. The feature from 400K to 800K at 60S is the strong Antarctic polar vortex mixing barrier (a similar picture for April shows a much weaker barrier in the Northern

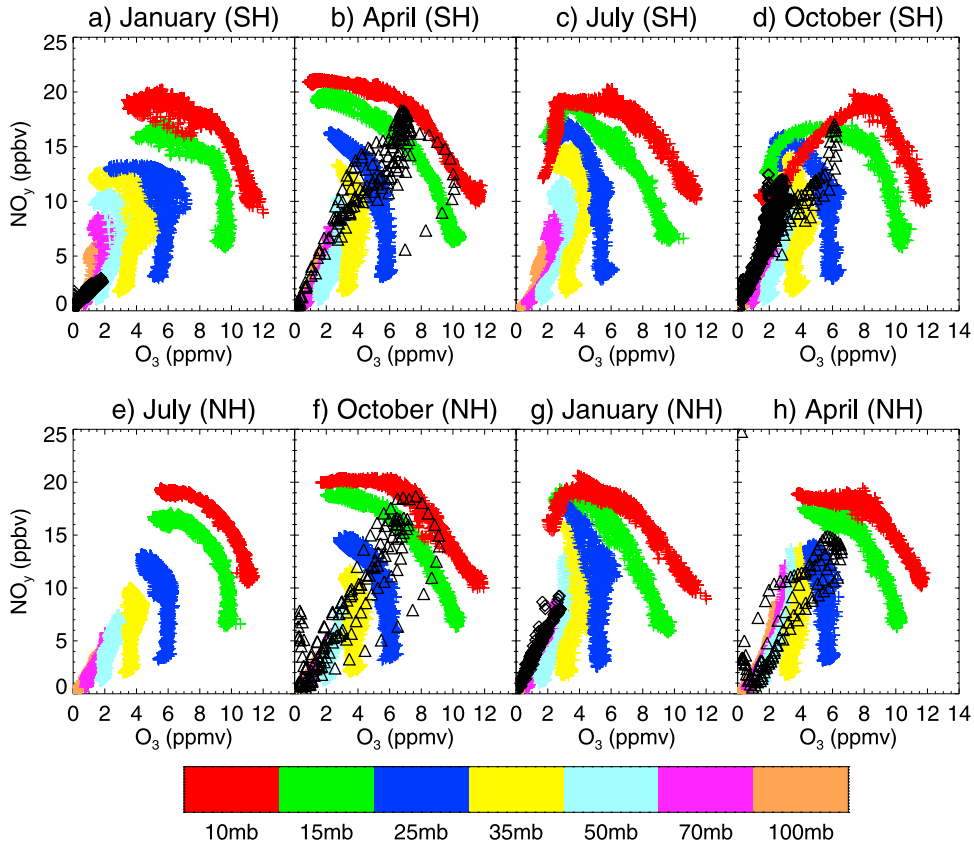

Figure 12. NO_y versus O_3 throughout the year. The correlations for the Southern Hemisphere (90S to the EQ) for (a) January, (b) April, (c) July and (d) October are shown in the top row. The correlations for the Northern Hemisphere (EQ to 90N) for (e) July, (f) October, (g) January and (h) April are shown in the bottom row. The pressure levels are color-coded as shown. The triangles show data from Figure 5 of *Michelsen et al.* [1998b] and the diamonds show data from Figure 3 of *Murphy et al.* [1993].

Hemisphere). Also clearly evident are the two edges of the tropical pipe at 20S and 30N. This is consistent with the correlation plots seen in Figure 7, which suggest that the data for 30S in Figure 7b lies along the midlatitude correlation curve, whereas in Figure 7c the correlation for 30N more closely resembles that of the tropical data. Although the tropical mixing barrier in the model may be weaker than in the real atmosphere, it clearly exists. Further evidence for the isolation of the tropics comes from the clear propagation of the tropical tape recorder signal well up into the CMAM upper stratosphere (see Figure 4 of *Shepherd* [2002]).

[28] The data from *Michelsen et al.* [1998b] have only limited spatial and temporal extent, because ATMOS is an occultation instrument with a short mission lifetime, but have excellent vertical coverage. It is therefore instructive to consider the extent to which the full hemispheric correlations from the model can be reproduced by limited sampling of the model data. The results from two such experiments are shown in Figure 10. Figure 10a shows the location of the Halogen Occultation Experiment (HALOE) sunrise sampling points for January 1992, with the correlations made by sampling CMAM data at these points shown in Figure 10b; the black points show the correlation from CMAM for the whole Northern Hemisphere, the red points show the correlation produced by sampling CMAM at the HALOE points over the whole month, and the yellow points show the correlation produced by sampling at the HALOE points on 16 January only. The full and limited correlations agree to some extent, but the slope of the correlation curve is slightly different in each case. At these latitudes HALOE is able to sample the tropical correlation, but only part of the midlatitude correlation. Figure 10c shows the simulated sampling points for the Atmospheric Chemistry Experiment (ACE) instrument, which is also an occultation instrument, in January 2003 (K. Walker, personal communication, 2002), and Figure 10d shows the correlations produced by sampling CMAM data at the ACE points with the color-coding as in Figure 10b. Although the latitudinal extent of the ACE samping is lower than that of HALOE (for these months), it is able to cover a much greater extent of the midlatitude correlation. This is due to the measurements at higher latitudes sampling a greater range of mixing ratios, because of the characteristic shape of the mixing ratio isopleths (Figure 1). Thus, for these two long-lived species, a limited sample can produce a good representation of the larger correlation picture, although one must be conscious of the measurement locations relative to any mixing barriers.

4.3. NO_y Versus N_2O

[29] Figure 11 shows the annual variation of the correlations between NO_y and N_2O for both hemispheres. The

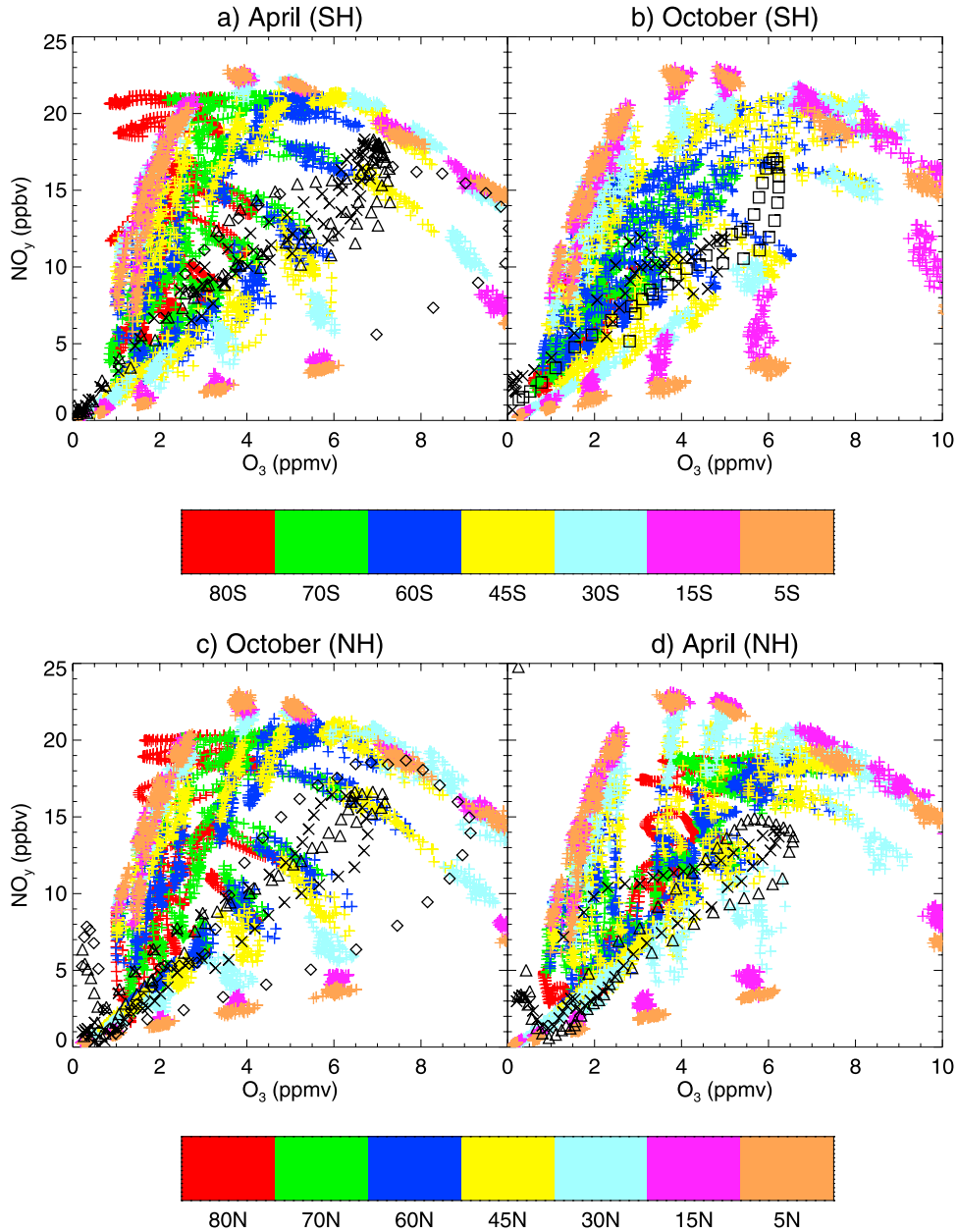

Figure 13. NO_y versus O_3 in the Southern Hemisphere for (a) April and (b) October, and in the Northern Hemisphere for (c) October and (d) April. The color-coding shows the latitude at which the vertical sections were taken. In the vertical the data lie between 100mb and 0.3mb. The black symbols represent data from Figure 5 of *Michelsen et al.* [1998b], with diamonds showing tropical data, squares showing midlatitude data, triangles high-latitude data, and crosses vortex data.

latitudinal extent of the data are identical to those in Figure 6. NO_y is the total reactive nitrogen, and is the sum of the mixing ratios of NO, NO_2, HNO_3, $2 \times N_2O_5$, and $ClONO_2$ [*Fahey et al.*, 1989]. Also shown in Figure 11 are ATMOS data from *Michelsen et al.* [1998b] and ER-2 data from *Strahan* [1999]. The former represent vertical profiles, while the latter represent horizontal profiles.

[30] The correlations shown here from the CMAM are in broad agreement with the 2D model results presented by *Plumb and Ko* [1992]. There are three distinct regions in each of the correlation plots. At low altitudes (between 100 and 35mb) there is a fairly compact correlation between the two species. In this region both tracers are long-lived compared to the quasi-horizontal mixing timescale. NO_y increases with altitude while N_2O decreases, reflecting the conversion from N_2O to NO_y. So the negative slope of the correlation results from chemistry, but as argued in section 2 the compactness of the correlation is due to mixing. At higher altitudes, however, the blue and yellow points show some evidence of spreading, and the compact correlation breaks down. At these altitudes the conversion of N_2O to NO_y is more rapid, meaning that at these altitudes the conditions for a compact correlation outlined in section 2 are violated. Higher still, above the source of NO_y the

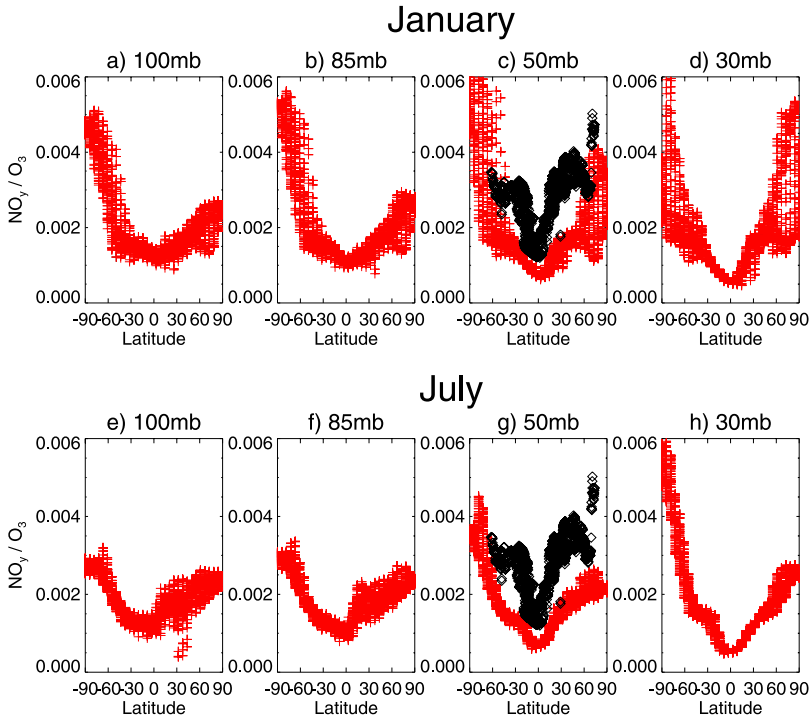

Figure 14. (a–h) NO_y divided by O_3 versus latitude on the 100mb, 85mb, 50mb and 30mb pressure surfaces on the first day of January (top row) and July (bottom row) in the 24th year of the model run. The red crosses show data from the CMAM, and the diamonds on the 50mb plots show data from Figure 5 of *Murphy et al.* [1993].

correlation again becomes compact because of the long lifetimes of both species in this region.

[31] The agreement between the model and the data is reasonable, although the model values of NO_y seem slightly higher at lower levels for all months. The model is unable to produce the very low values of NO_y shown in the *Michelsen et al.* [1998b] data for the vortex (Figures 11d and 11h). It was originally thought that these low values of NO_y were due to denitrification [*Rinsland et al.*, 1999], which is not included in the current version of the CMAM, but it is now widely accepted that an alternative explanation for the low NO_y is that air with lower NO_y mixing ratios is brought down from above and mixes with extravortex air [*Michelsen et al.*, 1998b] across the polar vortex barrier. The inference is then that the CMAM vortex confinement is either too strong (in the Antarctic) or too weak (in the Arctic) to exhibit the phenomenon.

4.4. O_3 Versus NO_y

[32] Correlations between O_3 and NO_y are shown in Figure 12 for both hemispheres. The gaps between the colors are due to the fact that the tracers have only been sampled at distinct pressure levels, because of the distinct vertical levels in the CMAM. With higher vertical resolution these gaps would fill in. The space-filling scatterplots result from the short lifetime of O_3 throughout most of the stratosphere. We can also see the effects of the region of rapid conversion from N_2O to NO_y descending in the winter months leading to the decrease in values of NO_y at 10mb at that time of year (Figures 12c, 12d, and 12g). Also shown in Figure 12 are ER-2 data from *Murphy et al.* [1993] (the diamonds in Figures 12a and 12g) and ATMOS data from *Michelsen et al.* [1998b] (the triangles in Figures 12b, 12d, 12f, and 12h). The correlations shown by these data suggest greater compactness than those produced by the model, an artifact of limited sampling. (As models are generally too diffusive compared to reality, they are likely to err on the side of overly compact correlations.) Figure 13 shows panels b, d, f, and h of Figure 12, but resampled by latitude. Again the data from *Michelsen et al.* [1998b] are shown and labeled by latitude (see figure caption for details). Sampling the model in this way highlights that the greatest variation in the correlation is produced in tropical latitudes. This is also shown in the data (the diamonds in Figures 13a and 13c). We can also see that the tropical correlation is clearly distinct from the midlatitude data, especially at lower altitudes (the low NO_y values of the orange and magenta points), but in fact the correlations are nowhere compact. The samples from higher latitudes exhibit much less variability, but even there the correlation is not compact.

[33] *Murphy et al.* [1993] have attempted to use this correlation (despite its lack of compactness) to investigate the transport of reactive nitrogen in the atmosphere, and found evidence for the existence of a subtropical mixing barrier. Because of such a subtropical barrier, the air parcels within the tropics are at least partially isolated from the air parcels on the midlatitude side of the mixing barrier, and hence there are two distinct regions of the correlation diagram. These can best be seen by plotting the ratio of NO_y/O_3 versus latitude, as shown in Figure 14. The ratio from *Murphy et al.* [1993] is also shown in Figures 14c and 14g. The data from Murphy et al. was taken at various times

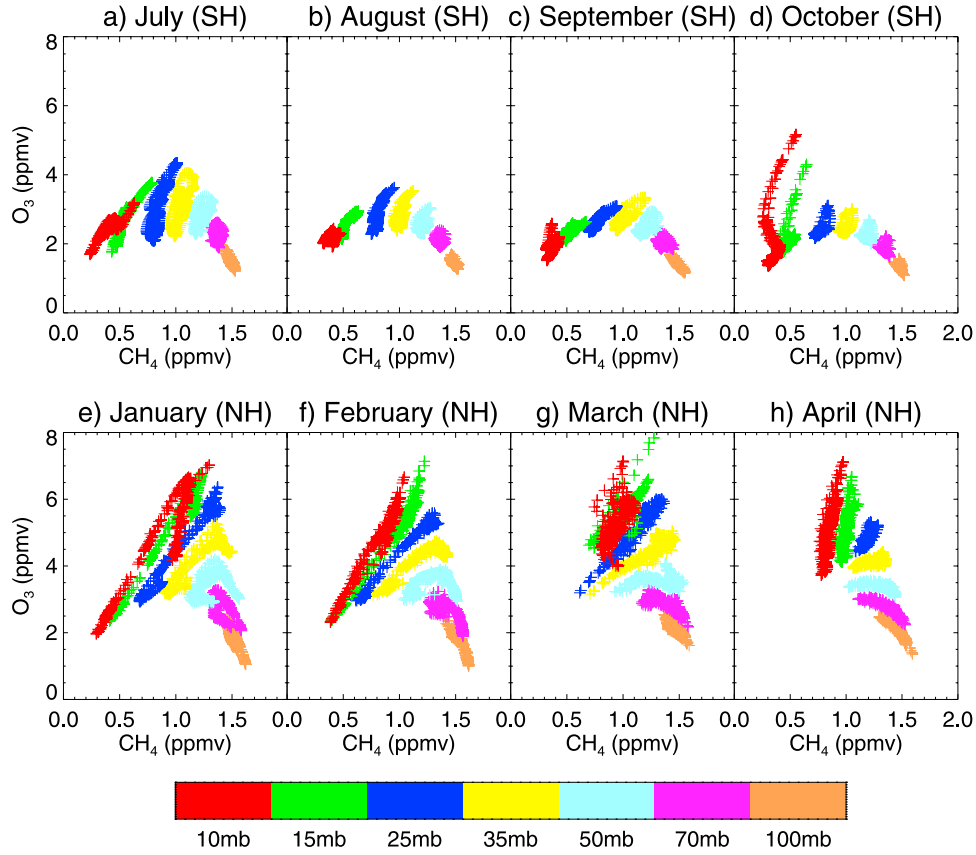

Figure 15. O_3 versus CH_4 throughout the winter/spring months of each hemisphere. The correlations for the Southern Hemisphere (90S to 70S) for (a) July, (b) August, (c) September and (d) October are shown in the top row. The correlations for the Northern Hemisphere (70N to 90N) for (e) January, (f) February, (g) March and (h) April are shown in the bottom row. The pressure levels are color-coded as shown.

throughout the year so the same ratio is shown in both panels. The results suggest that the tropical barrier in the CMAM certainly exists, although perhaps it is not as strong as in the real atmosphere, as evidenced by the sharper gradients in the observations from Murphy et al. For both these months the model shows that the distinction between tropical air (low values of the ratio) and extratropical air (high values of the ratio) is most clearly seen at the higher levels (50mb and 30mb). This is consistent with the idea that the tropical pipe edge is stronger at these levels. This agrees with the picture of the tropical mixing barrier seen in Figure 9, where the jump in the mixing ratio of N_2O is larger at higher altitudes. In contrast, lower down, around 100mb, the pipe is known to be "leaky" thus blurring the distinction between tropical and extratropical air parcels [*Volk et al.*, 1996].

4.5. O_3 Versus CH_4

[34] If data are taken throughout the stratosphere as a whole, correlations between O_3 and CH_4 appear very similar to those between NO_y and O_3; the greatest differences are that since there is no source of CH_4 in the stratosphere, the values of CH_4 do not decrease above 10mb in the winter months. As such, correlations between O_3 and CH_4 provide little information beyond what has already been noted.

[35] However, an interesting issue arises from the work of *Müller et al.* [1996]. They attempt to use correlations between O_3 and CH_4 to calculate chemical O_3 loss inside the Arctic polar vortex, by comparing correlations between these two species before and after springtime O_3 destruction has occurred. The argument is that because CH_4 is long-lived, it can be used as a parcel label and hence changes in O_3 at a given value of CH_4 correspond to chemical O_3 loss. Given that we expect the correlation between CH_4 and O_3 to generally be space-filling, it is interesting to investigate this issue further.

[36] The measurements used by *Müller et al.* [1996] are restricted in latitude range by the fact that sparse HALOE measurements are used and by the requirement that the measurements lie within the polar vortex. Figure 15 therefore shows correlation plots for O_3 versus CH_4 as they vary throughout the winter and spring months of year 24 of the CMAM run for points located close to the poles. Again one has to imagine the gaps being filled in reality. Figures 15a–15d show that although there is not a compact correlation between O_3 and CH_4 in July, one develops over the following months before beginning to break down again, particularly at the higher altitudes, in October. In the Northern Hemisphere, however, the four correlation plots show no evidence of compactness.

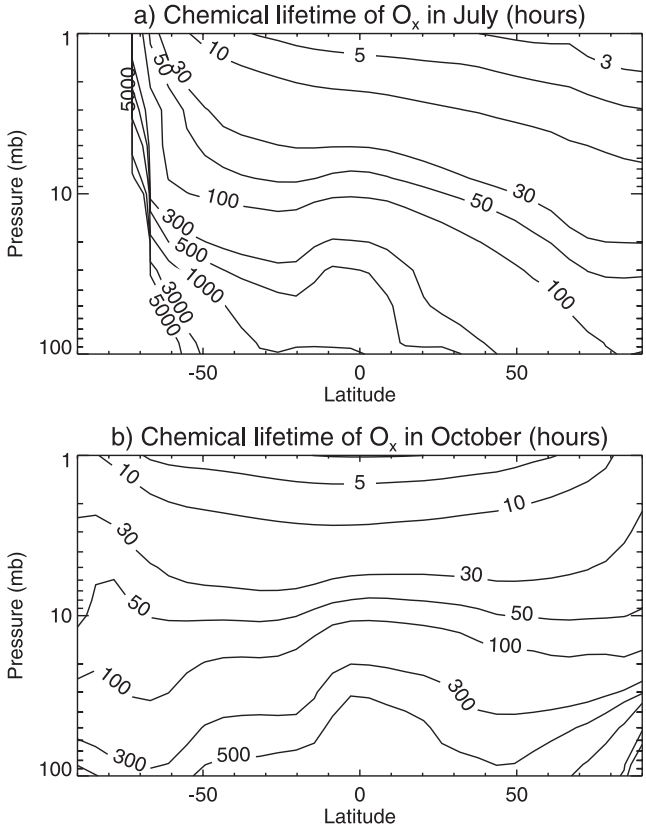

Figure 16. The chemical lifetime of O_x (hours) in the stratosphere for (a) July and (b) October calculated from the CMAM data. Note that the lifetime of O_x inside the Antarctic polar vortex during the winter months exceeds 5000 hours.

[37] When the polar vortex initially forms, the air parcels trapped inside do not exhibit a compact correlation, but instead reflect the global non-correlation of O_3 with CH_4. During the winter months, however, if the air parcels are trapped within the polar vortex, then they are not exposed to sunlight and O_3 within the vortex has a long chemical lifetime. Under such conditions, which are most likely to obtain in the Antarctic, we might expect a compact correlation to develop, although the process requires a finite time. Figure 15c shows the development of a compact correlation by September in the CMAM Antarctic. In contrast, the CMAM Arctic polar vortex appears to be sufficiently disturbed by extrapolar air to disrupt any correlation that might form over the dark winter months.

[38] Figure 16 shows the chemical lifetime of O_x for July (Figure 16a) and October (Figure 16b) calculated from the CMAM (O_3 and O are in a rapidly established photochemical equilibrium in the stratosphere, so $O_x = O + O_3$ is the relevant quantity affected by transport). The corresponding plots for January and April are not shown, but they are similar, the only difference being that they are reflected about the equator. The top plot in this figure shows clearly that O_x has a long lifetime within the Antarctic polar vortex during the dark winter months. By October, however, sunlight penetrates to high latitudes and O_3 is photochemically destroyed. This, however, is perhaps not enough to immediately destroy the correlation: If the air is sufficiently well trapped within the vortex then the correlation will be destroyed only slowly.

[39] To investigate the strength of the polar vortex barrier we have performed particle advection runs using a modified version of the contour advection code of *Dritschel* [1988]. Particles were set up in latitude bands 10 degrees apart from 80S to 30S on several isentropic (θ) surfaces and then advected diabatically for 10 days using the model winds and radiative heating rates. Figure 17 shows the distribution of the particles that started on the 700K surface ($\approx$25 km) after 10 days for July (Figure 17a) and October (Figure 17b). The left-hand panels show a plan view of the distribution, and the right-hand panels show the θ-level-latitude distribution. The results show that during July the air inside the Antarctic vortex is well confined and mixing occurs only in midlatitudes. In October, however, although the polar air still maintains much of its distinctiveness, the mixing at the high latitudes is more pronounced (for example, the green and yellow contours overlap). Also in October the midlatitude air is seen to reach much further poleward; in the height-latitude picture for October the magenta particles reach from the equator to 60S. It is this mixing-in of midlatitude air that produces the tail-like features on the correlation plots between CH_4 and O_3 at the higher altitudes (the red and green points in Figure 15d).

[40] Figure 18 shows a similar particle advection run for the Arctic performed for the first 10 days of January (Figure 18a) and April (Figure 18b). The plan views (on the left-hand side of the figure) show that indeed there is much greater mixing over the whole latitude range. Particles that originated in the midlatitudes have been able to mix all the way to the polar regions after only 10 days. It is for this reason that a compact correlation between CH_4 and O_3 cannot form during this CMAM year over the Arctic pole. This is consistent with the lack of a distinct Arctic CH_4:N_2O correlation for CMAM in Figure 7d.

[41] The effects of limited sampling of the polar vortex are illustrated by Figure 19, which shows a plot of the mixing ratios of O_3 versus CH_4 inside the Arctic vortex from the model in January, as well as the correlation produced by sampling from the HALOE points inside the vortex for January 1992 (chosen for illustrative purposes). During January 1992 HALOE sampled points inside the model vortex relatively infrequently, and even then only at the southernmost extent. If the only measurements we had were those from HALOE, then we might falsely think that a compact correlation existed. The same point applies for measurements taken at a single altitude (say from an aircraft). This figure highlights the importance of having enough data; given limited observations at a particular altitude or latitude, one could be under the erroneous impression that a compact correlation exists between two chemical species when in reality this is not the case.

4.6. CO_2 Versus N_2O

[42] *Boering et al.* [1994] have shown that the correlation between CO_2 and N_2O exhibits a strong seasonal variation in the lower stratosphere, the effect decreasing

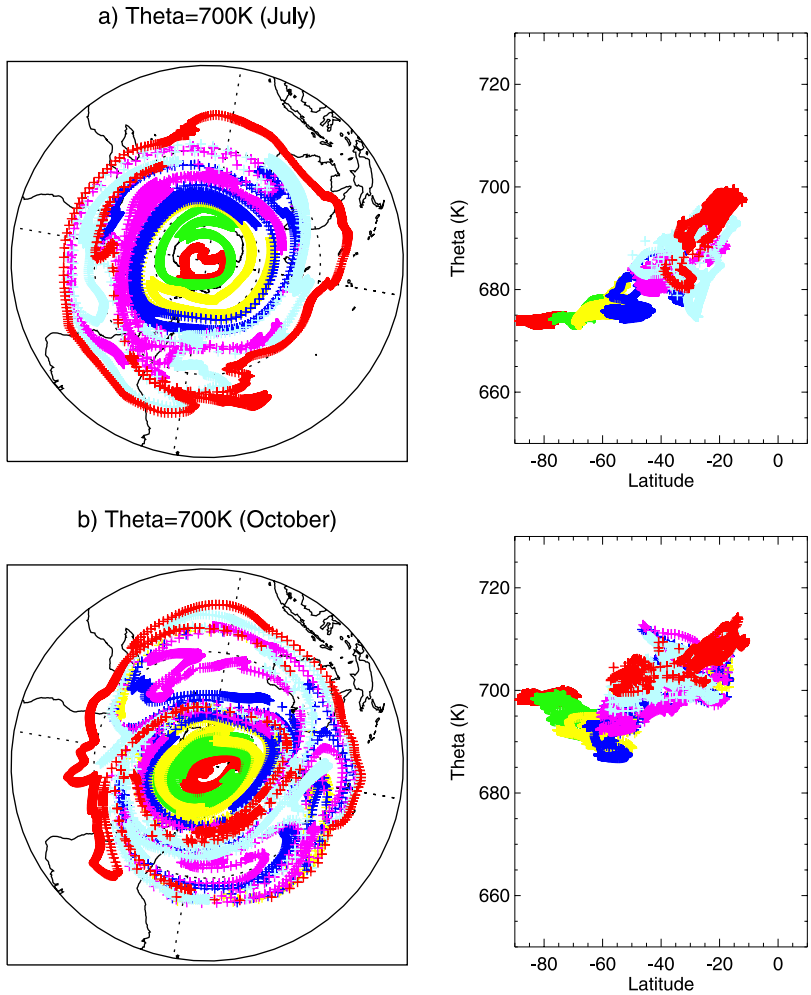

Figure 17. Distribution of particles after a 10 day advection run for (a) July and (b) October. The particles were initialized on latitude circles 10 degrees apart from 80S to 30S and on the 700K isentropic surface.

with increasing altitude. CO_2 is a long-lived tracer throughout the atmosphere, but its tropospheric values show a well-defined annual cycle, with low values in Northern Hemisphere fall and high values in Northern Hemisphere spring, because of the interhemispheric asymmetry of the land surface. An effect somewhat akin to the water vapor "tape recorder" [*Mote et al.*, 1996] permits this annual variation of the CO_2 mixing ratio to propagate up into the stratosphere.

[43] Although the CMAM run examined here does not have an annually varying CO_2, a separate run was performed to investigate if the seasonal variation of a CO_2-like correlation could be reproduced and if the effect decreased with increasing altitude. In the run, the CO_2-like tracer has a sinusoidally varying source at the surface with a period of one year. Similarly an N_2O-like tracer was set up with a constant source at the surface. Away from these surface sources the two tracers are advected in a passive manner. Figure 20 shows a correlation between the two tracers from year 9 of the run, as well as the observed correlations from *Boering et al.* [1994]. Although highly idealized, the results from the model are similar in character to those found observed in the data. At the higher altitudes (around 50mb) the shape of the correlation plot remains qualitatively similar between May and October. However at the lower altitudes, particularly around the 200 and 150mb levels, there is quite clearly a change in the sign of the gradient of the correlation curve between these two months. The effect of the seasonal variation propagates in phase and decreases in amplitude as one moves higher in the atmosphere. The signal appears to be about six months out of phase at 85mb. This oscillation of the correlation curve in time may be considered the "CO_2 tape recorder."

5. Conclusion

[44] Although it is impossible to cover all possible combinations of correlation plots between different chemical species in the atmosphere (or even in the CMAM), this paper has attempted to touch upon some of the more common ones used by various authors in recent years. Apart from helping to validate the model, the aim is to help understand the various factors that determine the structure of chemical correlation

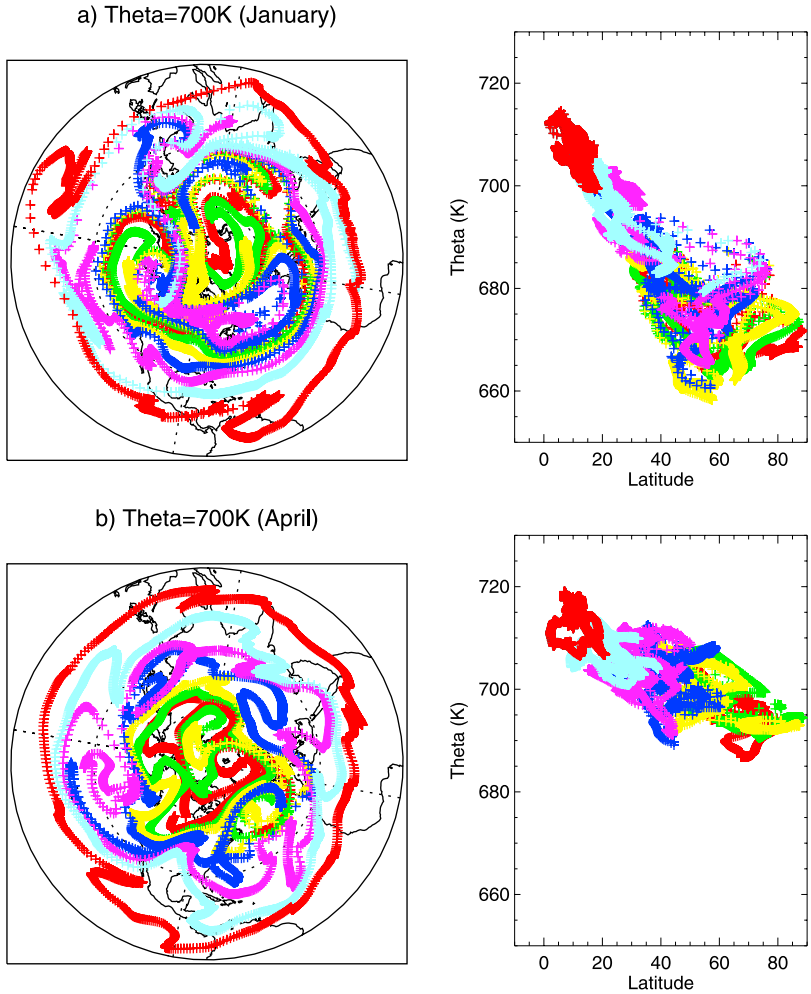

Figure 18. Distribution of particles after a 10 day advection run for (a) January and (b) April. The particles were initialized on latitude circles 10 degrees apart from 30N to 80N and on the 700K isentropic surface.

plots, as well as their seasonal evolution. Real measurements of chemical correlations are limited both spatially and temporally, and this work may enable such measurements to be used with greater confidence in the future.

[45] The effects that numerical methods employed by atmospheric models have on the formation and maintenance of compact correlations between chemical species have been considered by *Thuburn and McIntyre* [1997]. It was found in the present study that the correlations produced by the CMAM agree well with the theory of *Plumb and Ko* [1992], in that only those species with long lifetimes compared to the quasi-horizontal mixing timescale exhibit compact correlations with each other. It is impossible to get a perfectly compact correlation, and some "spreading" of the correlation always occurs; this is particularly evident in the striation patterns that occur in many of the correlation plots shown here. The striations are the result of an imperfect overlap of the two tracer mixing ratio isopleths, and are obtained for both horizontal and vertical sampling.

[46] The existence of mixing barriers in the atmosphere complicates the idealized correlations between chemical species considered by *Plumb and Ko* [1992]. *Plumb et al.* [2000] have shown how one would expect mixing barriers to produce anomalous correlations, and there is clear evidence for such anomalous correlations in the CMAM results shown here. For example, the existence of the tropical pipe mixing barrier leads to a different correlation in tropical regions than that seen in midlatitude regions (Figures 7 and 14). Although the tropical pipe mixing barrier in the CMAM may be slightly weaker than that in the real atmosphere, the distinction between the tropical and midlatitude correlations can nevertheless be quite clearly seen, and the location of the transition is consistent with the mixing barrier inferred from the tracer gradient (Figure 9).

[47] During the wintertime, the polar vortex edge can also produce anomalous correlations. This effect was highlighted by the correlation between N_2O and CH_4 in the Southern Hemisphere in November (Figure 8). The results from the CMAM exhibit these anomalous correlations only during the Southern Hemisphere winter and spring, because the simulated Arctic polar vortex is apparently always too weak to produce an effective mixing barrier. In the real

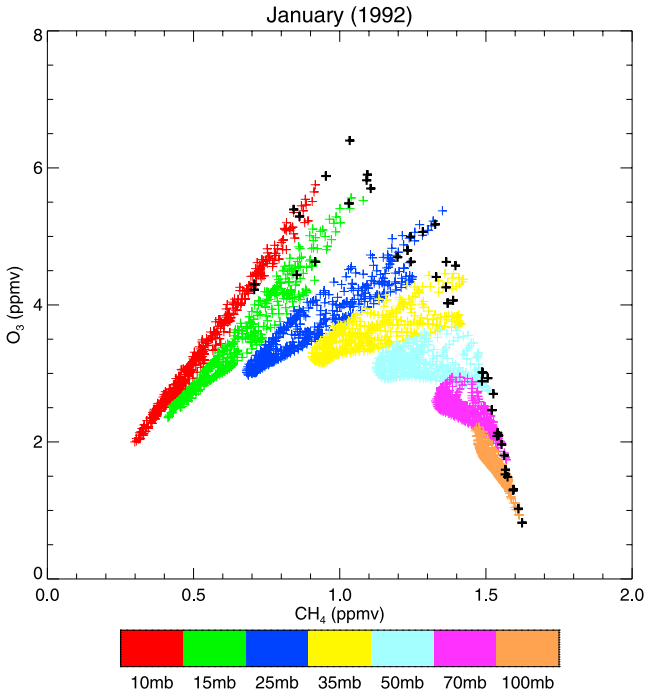

Figure 19. O_3 versus CH_4 for the first day of January in the Northern Hemisphere as in Figure 15e. The black points represent a sample taken by HALOE over the whole month of January 1992 to mimic the data from vertical soundings. Considered alone, the black points could lead to the misleading interpretation that a compact correlation exists between the two species.

atmosphere, however, it appears from measurements that anomalous correlations also occur in the Arctic wintertime, depending on the strength of the polar vortex in a given year.

[48] Using the CMAM has also allowed us to investigate the extent of data coverage required to adequately characterize a correlation. Limited sampling was shown not to be such a problem when dealing with long-lived species, where correlations are quite compact, at least within distinct regions. For the correlation between N_2O and CH_4 a reasonable representation of the midlatitude correlation can be obtained even from satellite sampling points that cover only a small range of latitudes. Similarly the measurements from a single day provide an adequate representation of the correlation as a whole. It was also shown that having a greater latitudinal coverage of data does not necessarily lead to a greater sampling of the midlatitude correlation curve. The smaller latitudinal extent of the simulated ACE data covered more of the correlation curve than the simulated HALOE data by virtue of its more northerly location, which allows sampling of a greater range of mixing ratios (Figure 10). The spatial extent of the data is nevertheless more important than the temporal extent since the correlations only vary slowly in time.

[49] In the case of correlations between O_3 and CH_4, a general lack of compactness is evident in the CMAM data (Figure 15). Using the CMAM data it would be impossible to use the method of *Müller et al.* [1996] to calculate chemical O_3 loss in the Arctic polar vortex, because the correlations are never compact. Even in the Antarctic, where compact correlations do develop by late winter, the "early vortex" correlation would need to be taken sufficiently late in the season to ensure it was compact. The CMAM results illustrate the fact that for short-lived species, limited satellite or ground-based measurements may lead to the erroneous conclusion that a well-defined compact correlation exists when in fact it does not. Thus correlations (especially those involving O_3) must be used with care; the method of *Müller et al.* [1996] may not be reliable for warm winters where the vortex is weak, or too early in the winter [*Salawitch et al.*, 2002].

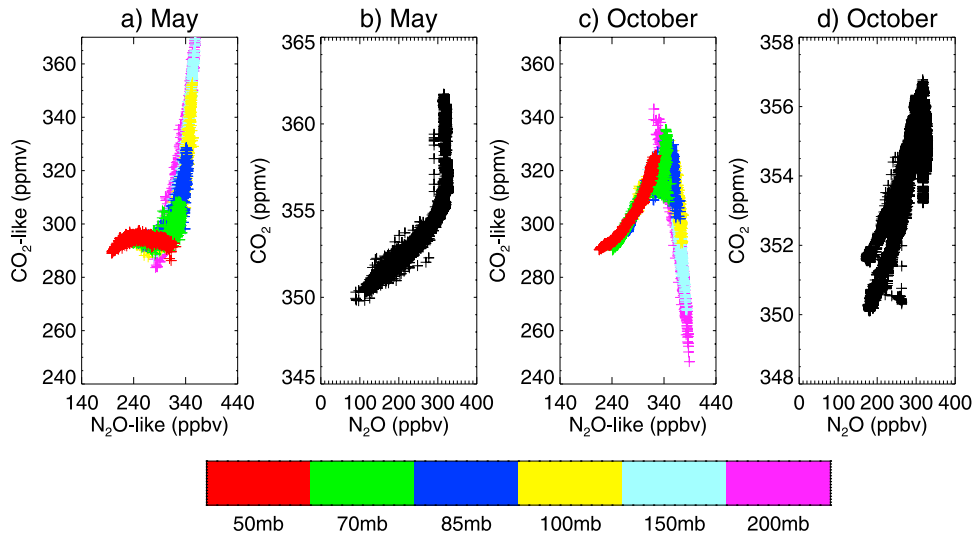

Figure 20. A CO_2-like versus an N_2O-like tracer for (a) May and (c) October for year 9 of a CMAM simulation. The latitudinal extent of the data runs from 10N to 70N. The pressure levels are color-coded as shown. (b) and (d) show observations taken from *Boering et al.* [1994] for May and October respectively.

[50] **Acknowledgments.** This research was supported by the "Modeling of Global Chemistry for Climate" project, with support from the Natural Sciences and Engineering Research Council, the Meteorological Service of Canada through its Climate Research Network, the Canadian Space Agency, and the Canadian Foundation for Climate and Atmospheric Sciences. The authors would also like to thank Kristie Boering, Hope Michelsen, Dan Murphy, and Susan Strahan for the provision of their data. Finally, we would like to thank the two anonymous reviewers for their helpful advice and suggestions.

References

Allam, R. J., K. S. Groves, and A. F. Tuck, Global OH distribution derived from general-circulation model fields of ozone and water-vapor, *J. Geophys. Res.*, *86*, 5303–5320, 1981.

Avallone, L. M., and M. J. Prather, Photochemical evolution of ozone in the lower tropical stratosphere, *J. Geophys. Res.*, *101*, 1457–1461, 1996.

Avallone, L. M., and M. J. Prather, Tracer-tracer correlations: Three dimensional model simulations and comparisons to observations, *J. Geophys. Res.*, *102*, 19,233–19,246, 1997.

Beagley, S. R., J. de Grandpré, J. N. Koshyk, N. A. McFarlane, and T. G. Shepherd, Radiative-dynamical climatology of the first-generation Canadian Middle Atmosphere Model, *Atmos. Ocean*, *35*, 293–331, 1997.

Boering, K. A., B. C. Daube, S. C. Wofsy, M. Loewenstein, J. R. Podolske, and E. R. Keim, Tracer-tracer relationships and lower stratospheric dynamics: CO_2 and N_2O correlations during SPADE, *Geophys. Res. Lett.*, *21*, 2567–2570, 1994.

de Grandpré, J., J. W. Sandilands, J. C. McConnell, S. R. Beagley, P. C. Croteau, and M. Y. Danilin, Canadian Middle Atmosphere Model: Preliminary results from the chemical transport module, *Atmos. Ocean*, *35*, 385–431, 1997.

de Grandpré, J., S. R. Beagley, V. I. Fomichev, E. Griffioen, J. C. McConnell, A. S. Medvedev, and T. G. Shepherd, Ozone climatology using interactive chemistry: Results from the Canadian Middle Atmosphere Model, *J. Geophys. Res.*, *105*, 26,475–26,491, 2000.

Dritschel, D. G., Contour dynamics/surgery on the sphere, *J. Comput. Phys.*, *79*, 477–483, 1988.

Ehhalt, D. H., E. P. Röth, and U. Schmidt, On the temporal variance of stratospheric trace gas concentrations, *J. Atmos. Chem.*, *1*, 27–51, 1983.

Fahey, D. W., K. K. Kelly, G. V. Ferry, L. R. Poole, J. C. Wilson, D. M. Murphy, M. Loewenstein, and K. R. Chan, In situ measurements of total reactive nitrogen, total water, and aerosol in a polar stratospheric cloud in the antarctic, *J. Geophys. Res.*, *94*, 11,299–11,315, 1989.

Hall, T. M., and M. J. Prather, Seasonal evolutions of N_2O, O_3, and CO_2: 3-dimensional simulations of stratospheric correlations, *J. Geophys. Res.*, *100*, 16,699–16,720, 1995.

Holton, J. R., A dynamically based transport parameterization for one-dimensional photochemical models of the stratosphere, *J. Geophys. Res.*, *91*, 2681–2686, 1986.

Kelly, K. K., et al., Dehydration in the lower Antarctic stratosphere during late winter and early spring, 1987, *J. Geophys. Res.*, *94*, 11,317–11,357, 1989.

Loewenstein, M., et al., New observations of the NO_y/N_2O correlation in the lower stratosphere, *Geophys. Res. Lett.*, *20*, 2531–2534, 1993.

Mahlman, J. D., H. Levy III, and W. J. Moxim, Three-dimensional simulations of stratospheric N_2O: Predictions for other trace constituents, *J. Geophys. Res.*, *91*, 2687–2707, 1986.

Michelsen, H. A., G. L. Manney, M. R. Gunson, C. P. Rinsland, and R. Zander, Correlations of stratospheric abundances of CH_4 and N_2O derived from ATMOS measurements, *Geophys. Res. Lett.*, *25*, 2777–2780, 1998a.

Michelsen, H. A., G. L. Manney, M. R. Gunson, and R. Zander, Correlations of stratospheric abundances of NO_y, O_3, N_2O and CH_4 derived from ATMOS measurements, *J. Geophys. Res.*, *103*, 28,347–28,359, 1998b.

Minschwaner, K., A. E. Dessler, J. W. Elkins, C. M. Volk, D. W. Fahey, M. Loewenstein, J. R. Podolske, A. E. Roche, and K. R. Chan, Bulk properties of isentropic mixing into the tropics in the lower stratosphere, *J. Geophys. Res.*, *101*, 9433–9439, 1996.

Mote, P. W., K. H. Rosenlof, M. E. McIntyre, E. S. Carr, J. C. Gille, J. R. Holton, J. S. Kinnersley, H. C. Pumphrey, J. M. Russell III, and J. W. Waters, An atmospheric tape recorder: The imprint of the tropical tropopause temperatures on stratospheric water vapor, *J. Geophys. Res.*, *101*, 3989–4006, 1996.

Müller, R., P. J. Crutzen, J.-U. Grooß, C. Brühl, J. M. Russell III, and A. F. Tuck, Chlorine activation and ozone depletion in the Arctic vortex: Observations by the Halogen Occultation Experiment on the Upper Atmosphere Research Satellite, *J. Geophys. Res.*, *101*, 12,531–12,554, 1996.

Murphy, D. M., D. W. Fahey, M. H. Proffitt, C. S. Liu, K. R. Chan, C. S. Eubank, S. R. Kawa, and K. K. Kelly, Reactive nitrogen and its correlation with ozone in the lower stratosphere and upper troposphere, *J. Geophys. Res.*, *98*, 8751–8773, 1993.

Plumb, R. A., A "tropical pipe" model of stratospheric transport, *J. Geophys. Res.*, *101*, 3957–3972, 1996.

Plumb, R. A., Stratospheric transport, *J. Meteorol. Soc. Jpn.*, *80*, 793–809, 2002.

Plumb, R. A., and M. K. W. Ko, Interrelationships between mixing ratios of long-lived stratospheric constituents, *J. Geophys. Res.*, *97*, 10,145–10,156, 1992.

Plumb, R. A., D. W. Waugh, and M. P. Chipperfield, The effects of mixing on tracer relationships in the polar vortex, *J. Geophys. Res.*, *105*, 10,047–10,062, 2000.

Proffitt, M. H., D. W. Fahey, K. K. Kelly, and A. F. Tuck, High-latitude ozone loss outside the Antarctic ozone hole, *Nature*, *342*, 233–237, 1989.

Proffitt, M. H., J. J. Margitan, K. K. Kelly, M. Loewenstein, J. R. Podolske, and K. R. Chan, Ozone loss in the Arctic polar vortex inferred from high-altitude aircraft measurements, *Nature*, *347*, 31–36, 1990.

Randel, W. J., J. C. Gille, A. E. Roche, J. B. Kumer, J. L. Mergenthaler, J. W. Waters, E. F. Fishbein, and W. A. Lahoz, Stratospheric transport from the tropics to middle latitudes by planetary-wave mixing, *Nature*, *365*, 533–535, 1993.

Rinsland, C. P., R. J. Salawitch, M. R. Gunson, S. Solomon, R. Zander, E. Mahieu, A. Goldman, M. J. Newchurch, F. W. Irion, and A. Y. Chang, Polar stratospheric descent of NO_y and CO and Arctic denitrification during winter 1992–1993, *J. Geophys. Res.*, *104*, 1847–1861, 1999.

Roach, W. T., Aircraft observations in the lower sub-arctic stratosphere in winter, *Meteorol. Res. Comm. Pap. 121*, U.K. Meteorol. Off., Bracknell, UK, 1962.

Salawitch, R. J., et al., Chemical loss of ozone during the Arctic winter of 1999/2000: An analysis based on balloon-borne observations, *J. Geophys. Res.*, *107*(D20), 8269, doi:10.1029/2001JD000620, 2002.

Shepherd, T. G., Issues in stratosphere-troposphere coupling, *J. Meteorol. Soc. Jpn.*, *80*, 769–792, 2002.

Strahan, S. E., Climatologies of lower stratospheric NO_y and O_3 and correlations with N_2O based on in situ observations, *J. Geophys. Res.*, *104*, 30,463–30,480, 1999.

Thuburn, J., and M. E. McIntyre, Numerical advection schemes, cross-isentropic random walks, and correlations between chemical species, *J. Geophys. Res.*, *102*, 6775–6797, 1997.

Volk, C. M., et al., Quantifying transport between the tropical and mid-latitude lower stratosphere, *Science*, *272*, 1763–1768, 1996.

D. Sankey and T. G. Shepherd, Department of Physics, University of Toronto, 60 St. George Street, Toronto, Ontario, Canada M5S 1A7. (sankey@atmosp.physics.utoronto.ca; tgs@atmosp.physics.utoronto.ca)